

# Enhancement of attachment of biomolecules on the surface of a blood vessel microchip under high blood flow rates

Subin Mao, Iqbal Kabir, and Long Que

**Abstract**— This paper reports on a new assay to enhance the immobilization of biomolecules on the surface of a blood vessel microchip, which will render the significantly improved binding of the biomolecules to the surface of the microfluidic channels, thereby allowing the studies of the behaviors of the biomolecules such as platelets under a broad range of flowing shear stresses from normal physiological to extreme pathological conditions.

## I. INTRODUCTION

In our recent studies, we have developed microfluidic chips designed to study platelet behavior by integrating microfluidic technology with molecular tension sensor [1]. These specialized chips feature integrin tension sensors (ITS) embedded within the inner surface of the microchannels, enabling the detailed integrin  $\alpha_{IIb}\beta_3$  force maps in platelets at a low flow condition (shear rates  $<100\text{ s}^{-1}$ ).

However, hemodynamic parameters that govern blood flow are known to significantly influence platelet-mediated thrombus formation, with shear rates in blood vessels ranging from 0 to  $4,600\text{ s}^{-1}$ , covering a spectrum from normal physiological to pathological conditions [2]. At high shear rates ( $>1,000\text{ s}^{-1}$ ), the ITS and consequently the platelets often cannot maintain adhesion within microfluidic channels due to enhance shear stress. This leads to their detachment and the removal of ITS from the channel surface under these conditions. This issue can be potentially addressed by a chemical surface functionalization process using APTES (3-aminopropyltriethoxysilane) and its linker, glutaraldehyde. This method can be adopted to enhance the adhesion of the ITS and thus the platelets to the surfaces of the microchannels by forming stable chemical covalent bonds with microchannel surface instead of physical adsorption [3], which is widely used, especially in fields such as biosensing [4-5], tissue engineering [6-7] for immobilization of protein and DNA [8-10], etc.

Herein, a surface functionalization process based on APTES chemistry has been developed to enhance the attachment of biomolecules on the surface of blood-vessel microchips with various dimension, thereby facilitating this method for studying platelets behavior under high blood flow in the future. For demonstration, Bovine Serum Albumin-Fluorescein Isothiocyanate (BSA-FITC conjugate) was used as fluorescence marker to evaluate the adhesion of the biomolecules on functionalized surfaces.

## II. MATERIALS AND METHODS

### Materials

**For microchip fabrication:** Negative photoresist SU-8 and SU-8 developer were purchased from MicroChemicals

\*Research supported by NSF ECCS# 2204447.

The authors are with the Department of Electrical and Computer Engineering, Iowa State University, Ames, IA 50011 USA, phone: 515-294-6951; e-mail: lque@iastate.edu.

(Germany). Polydimethylsiloxane (PDMS) and curing agents (SYLGARD™ 184 Silicon Elastomer Kit, 2-part) were purchased from Dow Corning (Midland, MI, USA). Glass substrates were purchased from Fisher Scientific (Hampton, NH, USA).

**For chemical surface functionalization of the microchip:** 3-aminopropyltriethoxysilane (APTES), the linker glutaraldehyde, and acetic acid solution were purchased from Sigma-Aldrich (St. Louis, MO, USA). Albumin from Bovine Serum (BSA), FITC conjugate was obtained from ThermoFisher (Waltham, MA, USA).

### Methods

#### Chip description and fabrication

The illustration of the blood vessel chip is schematically shown in **Fig. 1a**. Some micro-vessel structures in the chip were designed and fabricated to reflect the complexity of vascular system. Blood vessel system in the human body features a wide range of sizes from a diameter of about 25 mm for the aorta to only 8  $\mu\text{m}$  in the capillaries, adapted to various functions and location [11-12]. Multiple dimensions of microchips (from 150  $\mu\text{m}$  to 750  $\mu\text{m}$ ) have been designed and fabricated to assess the dimension effects on surface adhesive capability. The widths of the microchannel in the smallest chip vary from 150  $\mu\text{m}$  to 50  $\mu\text{m}$  while the height of all microchannel remains at constant.

The chip was fabricated using a soft lithography process. Briefly, a mold was first fabricated from negative photoresist SU-8. Mixture of polydimethylsiloxane (PDMS) base components and its curing agent in a 10:1 (w/w) ratio was poured on the mold followed by 2-hour degassing and 2-hour curing at 75°C. Thereafter, the PDMS replica of the microfluidic layer was peeled off from the mold, followed by the formation of the inlet and outlet by punching through PDMS layer using a biopsy punch. Finally, the microfluidic layer was bonded with a glass coverslip after plasma treatment to complete the fabrication of the chip. The blood vessel microchips of different dimensions have been fabricated to evaluate the effect of the flow rates on the modified surface.

#### Chemical surface functionalization

To enhance the adhesion between coverslip surface and integrin tension sensor (ITS), a surface functionalization process (**Fig. 1b**) was employed to create a silane layer using APTES and its linker glutaraldehyde.

Proper cleaning and surface activation of the glass (silicon) surface play key roles in the silane growth. First, the microfluidic chip was rigorously cleaned with acetone, IPA, and DI  $\text{H}_2\text{O}$ . Then the microchip underwent oxygen plasma treatment for 3 mins to remove impurities and organic contaminations from the channel surface. Plasma treatment controls surface hydrophilicity (increasing the

density of hydroxyl groups) to improve coating abilities with different chemical functional groups. After these cleaning steps, the microchip was ready for the silane attachment.

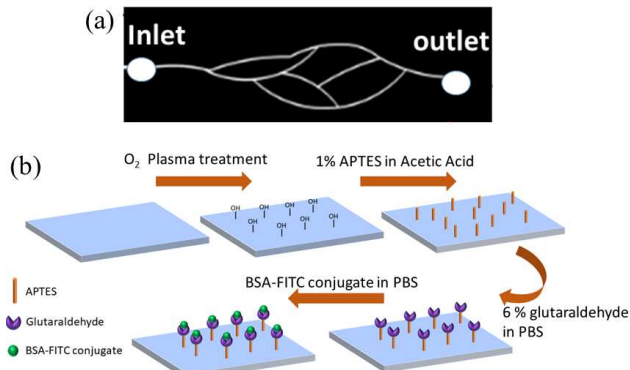


Fig. 1. (a) Schematic illustration of the microchip with blood-vessel structure; (b) illustration of the proposed surface functionalization process, oxygen plasma treatment is needed to increase the hydroxyl group on glass surface, improving the surface coating ability.

APTES was diluted in 1mM acetic acid (AA) to a concentration of 1% by volume. 1% APTES solution was injected into microchip, and the channel filled immediately due to surface hydrophilicity. The inner channel surface of the chip was left in contact with APTES solution for 2 hours at room temperature. The APTES-coated channel was then heated at 100°C for 1 hour to cure the silane layer, promoting the formation of siloxane bonds. A 6% glutaraldehyde solution in PBS was loaded into channel and incubated for 2 hours at room temperature [3]. The glutaraldehyde molecules interact with the amine group form APTES, forming imine bonds, which increase the stability of the linkage. Each step was followed by rigorously rinsing (3 times) using DI water.

Upon completion of the chemical surface functionalization, the microchip was ready for studying the effect of the shear rates in the range of 0 to 4600 s<sup>-1</sup>. In this demonstration, the BSA-FITC conjugate was used as the fluorescent tracer to assess surface adhesion. A solution of 0.1 mg/ml BSA-FITC conjugate in PBS was injected into the chip and incubated for 30 minutes under dark condition. Subsequently, DI H<sub>2</sub>O was flowed into chip using a syringe pump (Havard Apparatus, Inc.) at different flow rates, spanning from 5  $\mu$ l/min to 30  $\mu$ l/min, to evaluate the adhesion of the BSA-FITC conjugate on the surface of the microchannel through fluorescence imaging.

### Imaging

Brightfield images of the blood-vessel mimicking microchip and the fluorescence images of the BSA-FITC conjugate attached to channel surface were taken using Olympus ix73 inverted microscope (Olympus Corp. Tokyo, Japan) which equipped with standard epifluorescence illumination. A 4 $\times$  objective lens was used to obtain images for quantitative data analysis.

### Data acquisition and statistical analysis

ImageJ software (<https://imagej.net/ij/>) was used to

analyze and quantify images of the microchannel before and after flushing. The fluorescence intensity of the images was obtained using measurement tool in ImageJ. The observed fluorescence signals were adjusted to account for the background fluorescence. Origin (data analysis software, OriginLab Corporation) was used for statistical analysis and graph-plotting. The analysis of the microchannel fluorescence was based on at least three independent experiments, and at least ten spots on a single chip have been measured. All measurements are reported with standard deviation (mean  $\pm$  SD).

### III. EXPERIMENTAL SETUP AND PROCEDURES

Microchips with three different dimensions (width of inlet/outlet: 150  $\mu$ m, 300  $\mu$ m, and 750  $\mu$ m) have been fabricated to evaluate the effects of shear rate in the range of 0 to 4600 s<sup>-1</sup>. The process of surface functionalization involved injecting chemicals into microchip through the inlet at a controlled, low flow rate using a syringe coupled with a syringe pump. These steps were carried out in a fume hood.

Following the surface functionalization, the microchannels in each microchip were rinsed with DI H<sub>2</sub>O at precisely controlled flow rates of 5, 10, 15, 20, 25, and 30  $\mu$ l/min, generated by the syringe pump. After rinsing, the microchips were immediately prepared for imaging under a fluorescence microscope to assess the effectiveness of the functionalization.

### IV. RESULTS

We experimentally assessed and validated the adhesion properties of the substrate surface both before and after implementing the proposed surface functionalization process. The blood-vessel mimicking microchips, fabricated on glass coverslips in various dimensions as shown in Fig. 2, utilized a process developed in our lab [1]. The widths of the vessel microstructures inside these microchips range from the smallest size with a 150  $\mu$ m width at the inlet/outlet (Fig. 2b) to the largest size with a 750  $\mu$ m width at the inlet/outlet (Fig. 2c).

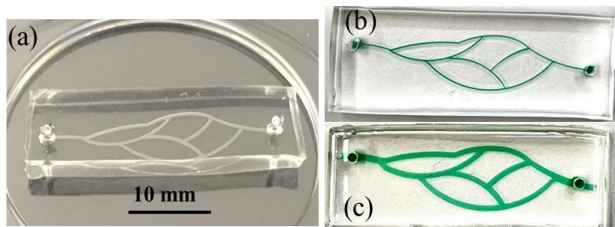


Fig. 2. (a) Photos of the fabricated blood vessel microchip showing complexity of vascular system; green dye indicating different dimensions of the microchips, (b) microchip with 150  $\mu$ m width at inlet/outlet; (c) microchip with 750  $\mu$ m width at inlet/outlet.

As anticipated, on the unfunctionalized surface, the BSA-FITC conjugate was readily washed away, even at a low flow rate. Fig. 3 shows the fluorescence images of the microfluidic channel (i.e., vessel) before and after the introduction of DI water at a flow rate of 20  $\mu$ l/min in an unfunctionalized blood vessel microchip. The images in Fig. 3c and 3d show an extremely weak fluorescence signal, indicating poor retention of BSA-FITC conjugate. In the

case of the microchip lacking chemical surface functionalization, over 95% of the BSA-FITC conjugate, as shown in **Fig.5a**, was easily rinsed away due to insufficient adhesion to the channel surface.

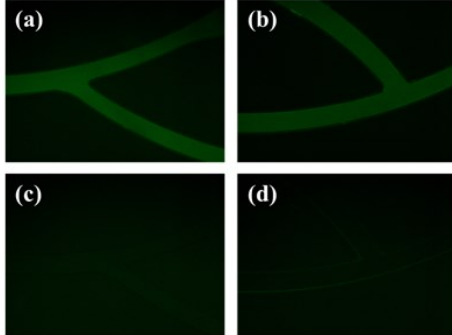


Fig.3. Fluorescence images of the microchannel without surface functionalization. (a-b) fluorescence images of the vessel structure before washing step; (c-d) corresponding fluorescence images after washing step.

Fluorescence signals were recorded before and after the washing step in the surface functionalized microchip. As shown, the initial fluorescence signals (**Fig. 4 a-c**) were observed with high intensity; even after washing step, the signals (**Fig. 4 d-f**) could still be detected at a reduced intensity. **Fig. 5b** shows significantly improved adhesion properties. Notably, at least 53.7% of the BSA-FITC conjugate remained adhered to the channel surface of the medium-size microchip, even the flow rate was up to 30  $\mu\text{L}/\text{min}$ , which verifies the effectiveness of surface functionalization in maintaining the attachment of the molecules under dynamic flow conditions, thus demonstrating the reliability of the chemical modifications applied to the substrate surface.

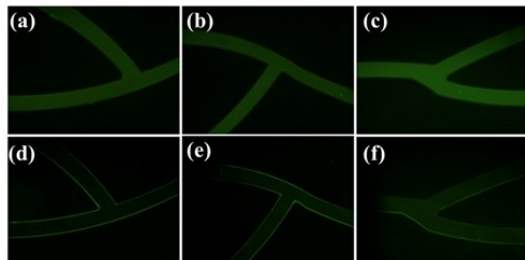


Fig.4. Fluorescence images of the microchannel with surface functionalization. (a-b) fluorescence images of the vessel structure before washing step; (c-d) corresponding fluorescence images after washing step.

Fluorescence intensity is determined by the shear rate, and the average shear rate depends on the several factors, including the volumetric flow rate, the cross-sectional area perimeter, and the shape factor of the microchannel. We examined the fluorescence signal at different flow rates and dimensions of the microchips. The calculation of shear rate in a rectangular channel is given by [13]:

$$\dot{\gamma} = \frac{QP\lambda}{8A^2}$$

where  $Q$  is the volumetric flow rate,  $A$  is the cross sectional area of the microchannel and  $P$  is the perimeter, and the shape factor  $\lambda$  is given by:

$$\lambda = \frac{24}{\left[ \left( 1 - 0.351 \frac{h}{w} \right) \left( 1 + \frac{h}{w} \right) \right]^2}$$

with  $h$  representing the height of the microchannel and  $w$  representing the width of the microchannel.

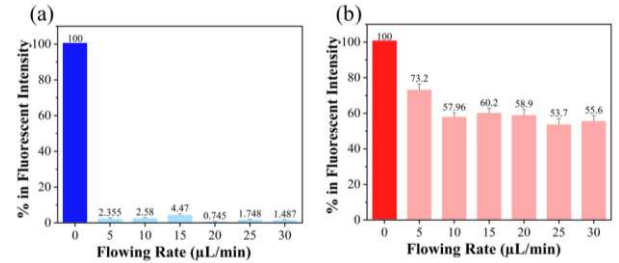


Fig.5. Quantified fluorescence intensity in % after flowing DI water with different flow rates. The percentage of the fluorescence signal remained after washing step in (a) un-functionalized microchips, and (b) functionalized microchips.

**Table. 1** presents the calculated shear rates for microchips of varying dimensions, under a ranges of volumetric flow rates from 5-30  $\mu\text{L}/\text{min}$ . The results indicate that the shear rate vary from  $154 \text{ s}^{-1}$  to  $2045 \text{ s}^{-1}$ . This calculation demonstrates that increases in volumetric flow rates or reductions in cross-sectional area of the microchips lead to higher shear rates. This trend shows the direct influence of flow dynamics and microchip geometry within microfluidic environments.

Flow rate ( $\mu\text{L}/\text{min}$ )	Shear rate ( $\text{s}^{-1}$ )		
	Small chip (150 $\mu\text{m}$ )	Medium Chip (300 $\mu\text{m}$ )	Large Chip (750 $\mu\text{m}$ )
5	340.74	160.32	154.41
10	681.50	320.65	308.82
15	1022.22	480.97	463.22
20	1362.83	641.23	617.56
25	1703.71	801.62	772.03
30	2044.44	961.94	926.43

Table.1 Calculated shear rates of different dimensions and various volumetric flow rates.

The measured fluorescence intensities on different microchips are shown in **Fig. 6** using ImageJ [14]. It has been observed that when volumetric flow rates or shear rates raised, the fluorescence intensities decreased, indicating some of the biomolecules were washed away. This scenario occurred since shear stress partially broke the link between BSA-FITC molecules and microchannel surface, while surface functionalization kept the majority of the chemicals and molecules attached to the surface.

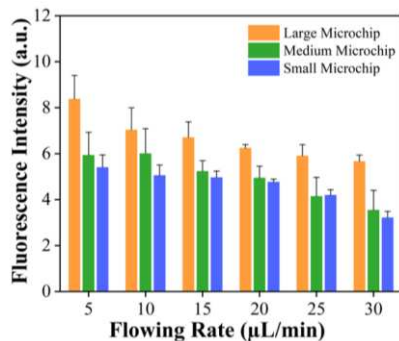


Fig.6. Measured fluorescence signals from surface functionalized microchips after washing step with varied flow rates.

**Fig.7** illustrates the effects of varying shear rates or volumetric flow rates (ranging from 5  $\mu\text{L}/\text{min}$  to 30  $\mu\text{L}/\text{min}$ ) on fluorescence signals from microchips with different dimensions. The quantified fluorescence intensity indicates that large microchips consistently produced higher signals compared to medium and small-size chips. The disparity in intensity can be attributed to several factors. The microchips with larger dimensions (i.e., larger microchannels) have a larger surface area that allows for more extensive interaction with and adherent of the chemicals/biomolecules, thus enhancing the fluorescence signal. In contrast, the microchips with smaller dimensions (i.e., smaller microchannels) result in a challenging microenvironment for the stability of chemicals attachment. The BSA-FITC conjugate molecules as fluorescent marker were more easily washed away in smaller microchannels. It is due to the higher shear rate/stress within smaller microchannels than that in larger microchannels for the same volumetric flow rates. A higher shear rate/stress lead to increased forces acting on the molecules and the bonds between them and microchannel surface. Consequently, this would make the bonds between chemicals/molecules and surface more prone to rupture.

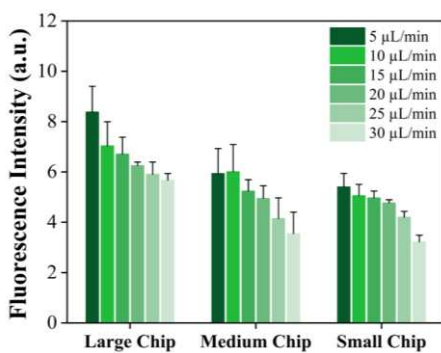


Fig.7. Comparasion of the fluorescence intensities within different microchips under different flow rates.

As demonstrated, the assay developed in this study can significantly improve the adhesion between microchannel surface and biomolecules, which will be adopted to study the behaviors of platelets by integrin tension sensors under different flow rates using the blood vessel microchip. This is crucial for assessing how platelets respond to various levels of shear stress ranging from normal physiological

conditions to those in pathological states, thereby mimicking the vascular environment more accurately.

## SUMMARY

The study successfully demonstrated the enhanced adhesion of biomolecules on blood vessel microchips through a surface functionalization process using APTES and its linker glutaraldehyde for surface functionalization, addressing the stability of biomolecules bonds across a wide range of shear rates. By modifying the dimensions of the microchips, it also revealed how microchannel sizes impacted biomolecules adhesion. Increased fluorescence signals or retention of BSA-FITC conjugates at higher flow rates validated the effectiveness of the surface treatment, verifying its potential for studying the effects of shear stress on platelets under high flow rates/shear rates.

## REFERENCES

- [1] S. Mao, A. Sarkar, Y. Wang, C. Song, D. LeVine, X. Wang, and L. Que, "Microfluidic chip grafted with integrin tension sensors for evaluating the effects of flowing shear stress and ROCK inhibitor on platelets," *Lab on a Chip*, 2021, 21, pp. 3128-3136.
- [2] K. Sakariassen, L. Orning, and V. Turitto, "The impact of blood shear rate on arterial thrombus formation," *Future science OA*, 1, no. 4, 2015.
- [3] G. Naga Siva Kumar, et al. "Optimization and characterization of biomolecule immobilization on silicon substrates using (3-aminopropyl) triethoxysilane (APTES) and glutaraldehyde linker," *Applied Surface Science*, 305 (2014): 522-530.
- [4] W. Wang, Y. Wang, L. Tu, T. Klein, Y. Feng, & J.P. Wang, (2012). Surface modification for protein and DNA immobilization onto GMR biosensor. *IEEE transactions on magnetics*, 49(1), 296-299.
- [5] M. Antoniou, D. Tsounidi, P. Petrou, K. Beltsios, & S. Kakabakos. (2020). Functionalization of silicon dioxide and silicon nitride surfaces with aminosilanes for optical biosensing applications. *Medical Devices & Sensors*, 3(5), e10072.
- [6] M.L. Foglia, et al. "A new method for the preparation of biocompatible silica coated-collagen hydrogels," *Journal of Materials Chemistry B*, 1, 45 (2013): 6283-6290.
- [7] B. Mahendiran, et al. "Surface modification of decellularized natural cellulose scaffolds with organosilanes for bone tissue regeneration," *ACS Biomaterials Science & Engineering*, 8, 5 (2022): 2000-2015.
- [8] G. Zhang, et al. "The immobilization of DNA on microstructured patterns fabricated by maskless lithography," *Sensors and Actuators B: Chemical*, 97.2-3 (2004): 243-248
- [9] Z. Wang, and J. Gang. "Covalent immobilization of proteins for the biosensor based on imaging ellipsometry," *Journal of immunological methods*, 285.2 (2004): 237-243.
- [10] E. Vandenberg, et al. "Protein immobilization of 3-aminopropyl triethoxy silane-glutaraldehyde surfaces: Characterization by detergent washing," *Journal of colloid and interface science*, 143.2 (1991): 327-335.
- [11] "Structure and Function of Blood Vessels." *Anatomy and Physiology II*, Lumen Learning. Accessed June 20, 2024. <https://courses.lumenlearning.com/suny-ap2/chapter/structure-and-function-of-blood-vessels>
- [12] "Blood Vessels." *Encyclopedia.com*, n.d. Accessed June 20, 2024. <https://www.encyclopedia.com/medicine/anatomy-and-physiology/anatomy-and-physiology/blood-vessels>.
- [13] C. Miller. "Predicting non-Newtonian flow behavior in ducts of unusual cross section," *Industrial & Engineering Chemistry Fundamentals* 11.4 (1972): 524-528.
- [14] X. Li, Y. He, and L. Que, "Fluorescence detection and imaging of biomolecules using the micropatterned nanostructured aluminum oxide," *Langmuir*, 29(7), 2439-2445 (2013).